JOURNAL OF MATERIALS SCIENCE 31 (1996) 2291–2299

Structural and residual stress changes in Mo/a-Si multilayer thin films with annealing

M. E. KASSNER, F. J. WEBER
Department of Mechanical Engineering, Oregon State University, Corvallis, OR 97331, USA
J. KOIKE
Department of Materials Science, Tohoku University, Sendai 980 Japan
R. S. ROSEN
Lawrence Livermore National Laboratory, Livermore, CA 94550, USA

The thermal and mechanical stability of molybdenum and amorphous silicon (Mo/a-Si) optical multilayers (3 and 4 nm nominal thickness of Mo and Si) at 316 °C were studied by annealing experiments. Growth of amorphous Mo–Si interlayers with a stoichiometry of 1:2 was observed at the Mo/a-Si interfaces. In addition, residual stresses significantly changed in the crystalline Mo and amorphous Si layers with annealing. High resolution electron microscopy, selected area electron diffraction, and X-ray diffraction of the crystalline Mo revealed that tensile stresses increased from 2 to about 10 GPa in the lateral direction (parallel to the interface plane). The compressive strains that developed in the vertical direction (perpendicular to the interface plane) are consistent with Poisson's ratio. Laser deflectometer measurements of thicker (0.1 μm) amorphous silicon layers may indicate compressive-stress relaxation in the amorphous silicon with annealing, consistent with other investigations. Overall, the residual stress in a 40-bilayer film changes from about − 0.5 to about + 1.5 GPa. Structural transformation after relatively short annealing times at the interfaces in the thin amorphous Mo–Si interlayers may rationalize increased tensile strains in the Mo layers.

1. Introduction

Extreme ultraviolet (EUV) reflecting mirrors can be made from a series of thin-film bilayers. One layer of the bilayer has a high atomic scattering factor while the other a low scattering factor. Molybdenum/amorphous silicon (a-Si) multilayers are an example of high reflectivity EUV mirrors. The reflectivity of these multilayered films is greatly affected by the interfaces between the layers. Ideal interfaces are flat with an abrupt composition change from one layer to the other. Roughness of the interface and interdiffusion between the layers degrade the reflectivity. Also, changes in the bilayer thickness due to interdiffusion modifies the X-ray wavelength at which peak reflectivity is achieved [1].

A Mo/a-Si 40-bilayer film with 3 nm Mo, 4 nm a-Si, and ideal interfaces would have a theoretical peak reflectivity of about 70 per cent for EUV of 13 nm wavelength at normal incidence. The actual reflectivity is about 66 per cent, reduced at least partly due to the formation of amorphous interlayers, during deposition, with a Mo:Si stoichiometry of about 1:2. Annealing the multilayers at temperatures up to 300–400 °C causes growth of the interlayers and their eventual crystallization, leading to further degradation of the reflectivity [2, 3]. This study will characterize changes in the structure with elevated-temperature exposure.

Furthermore, thin films are often in a state of high residual stress. This may disfigure the mirror or cause cracking of the film. Microstructural changes during annealing are expected to alter the stress state in multilayers. Some residual stress measurements on Mo/a-Si multilayers with relatively "*thick*" individual layers have been performed by Kola *et al.* [4]. The stress in the films was determined using laser deflectometry which measures the change in curvature of substrates that are relatively thick. This procedure, however, is generally used on relatively thick deposited layers (e.g. > 100 nm) and not on thin layers (< 5 nm). As the residual stresses may depend on the thickness of the crystalline layers, other techniques may be useful for optical multilayers. The defect structure and stress state may change in crystalline materials as the thickness increases beyond roughly 5 nm (larger than the layers in the multilayers of this study) due to the activation or mobility of misfit dislocations [5]. Thus, thick crystalline layers may plastically deform by dislocation motion resulting in residual stress states lower than those in multilayers with the layer thicknesses of this investigation. Furthermore, Nguyen and co-workers [6, 7] suggested that the

0022–2461

structure of a film may change with thickness, thus changing the average residual stresses. Thus, the conclusions of stress relaxation in crystalline phases with annealing by Kola *et al.* [4] may not be applicable to optical-scale multilayers.

The elastic strains can be determined in relatively thin layers (e.g. < 5 nm) using high resolution electron microscopy (HREM), selected area electron diffraction (SAED), and X-ray diffraction (XRD) for crystalline materials. XRD has been used by others on thin-layer multilayers [8] whereas the other techniques are less commonly used. Film stresses may be calculated from the obtained strains assuming that the elastic properties of the film are accurately known. Of course, diffraction methods cannot be used for residual stress measurements in amorphous materials. However, laser deflectometry can be used on thicker films to infer stresses in thin (e.g. 3 nm) films, assuming no thickness effects on amorphous film structure and, hence, residual stresses. As will be discussed later, these structural effects in amorphous as well as in crystalline materials may be avoided using a layering technique described by Nguyen [6]. Additionally, average stresses in optical multilayers (e.g. 40 bilayers of 3 nm Mo and 4 nm Si) can be reliably determined by laser deflectometry. Knowledge of the average stresses in the multilayer, Mo, and the thin amorphous silicon layers can thus be used to infer the residual stresses in the $MoSi_2$ interlayer. Thus, diffraction and laser deflectometry techniques may be used in a complementary manner for the characterization of the stress state in optical multilayers as a function of time at elevated temperature in this study.

This study investigated the thermal stability of reflective Mo/a-Si multilayers by examining changes in the microstructure and stress state during annealing at 316 °C, complementing earlier preliminary structural studies by the authors at other temperatures [1, 2]. Attempts were made to relate residual stress and microstructural alterations with elevated temperature exposure.

2. Experimental procedure

The multilayers of this study that were used for EUV mirrors consisted of 40 bilayers of Mo/a-Si consisting of nominally 3 nm Mo and 4 nm a-Si deposited on (1 0 0) oriented single crystal silicon wafers. The native oxide on the wafers was not removed. The deposition was performed using a d.c. magnetron sputtering system detailed elsewhere by the authors [9]. Argon was used as the sputtering gas.

Three, relatively thick mono-, bi-, and trilayered films were also deposited for additional laser diffractometer curvature measurements [a-Si, Mo on a-Si (or Mo/a-Si), and a-Si on Mo/a-Si or (a-Si/Mo/a-Si)]. Layers of about 0.1 μm (Si was 0.11 μm and Mo was 0.105 μm) were deposited on 350 μm thick, 100 mm diameter (whole), silicon single crystal wafers (⟨1 0 0⟩ perpendicular to the crystal surface). The deposition conditions for the thick and thin multilayers were identical, except that the increased thickness was achieved by multiple passes over a given sputtering target. Thicknesses for these were not measured but were assumed to be equal to the earlier confirmed thin-film thickness multiplied by the number of passes used to produce the thick film. These thicker layers were produced, principally, to determine residual stresses in a-Si optical multilayers. The background partial pressure is about 3×10^{-7} torr. This means that a monolayer of water may be absorbed on the surface during 10 s pass intervals. Therefore, there was concern that the thick-film data in this work is not necessarily reflective of pure material of identical thickness. However, Nguyen [6], with a similar working pressure, did not conclude such effects. In fact, this investigator appears to suggest that such a "layering" technique, for a pure material, such as Mo, is a means to maintain the structure of thin (nm-scale) films in thicker (μm-scale) films. Nguyen presents evidence that over the thickness range of about 5 nm to 1 μm without "layering", a-Si residual stresses may change by about a factor of two for "single" films. This is not a dramatic change and our "layering" or multi-pass technique may minimize this effect.

The optical multilayers used for the thermal stability study and examined by HREM, SAED and XRD were cleaved into relatively small (approximately 12 mm × 24 mm) sections and annealed for various periods at 316 °C, up to 100 h. They were sealed in Pyrex tubes and evacuated to less than 10^{-5} torr to minimize oxidation during annealing. The whole wafers used for curvature measurements at Stanford University were annealed at 316 °C for 0.5 h and 10 h. Since these wafers were 100 mm in diameter, the encapsulating tubes were relatively large (approximately 100 mm diameter and 300 mm length). Thus the time to reach 316 °C was longer, approximately 15 min as compared to about 5 min for the smaller samples. This increased the uncertainty of the 0.5 h annealing time for the whole wafers relative to that of the cleaved specimens. The cleaved (15 mm × 5 mm) wafers used for curvature measurements at Tohoku University in Sendai, Japan, were annealed at 316 °C for 0.33, 0.67, 1, 5, and 25 h. Specimens were annealed at 10^{-7} torr.

Specimens examined using HREM and SAED were mechanically polished, ion milled to perforation using a Gatan model 600 dual ion mill, and then examined with a JEM 4000 EX transmission electron microscope located at Arizona State University. The substrate was not removed so as to preserve mechanical constraint by the Si wafer. Mo–Si interlayer thickness changes due to growth during annealing were determined using high resolution lattice fringe images that were recorded on photographic plates, digitized and converted to 256 grey-scale images. The layers and interlayers could then be identified by their range of grey-scale values. A single colour was assigned to each range to aid in thickness measurements, which were performed at several locations in each image.

The {1 1 0} and {1 0 0} plane spacings were measured to determine lateral (parallel to the layers) and {1 1 0} vertical (perpendicular to the layers) strains in the Mo. The polycrystals of Mo were oriented (textured) such that ⟨1 1 0⟩ directions were parallel to the

multilayer normal. The lateral spacings were measured using conventional SAED. An entire multilayer was included in the aperture for the SAED pattern. This resulted in strong superlattice spots aligned in the vertical direction, which overlapped the transmission spot. Each crystalline spot had an intensity streaked in the vertical direction due to the effect of Mo layer thickness on the diffraction-intensity distribution. Therefore, the lateral diffraction pattern spacing, but not the vertical spacing, could be accurately measured using SAED. The {1 1 0} and {1 0 0} lattice spacings were obtained from the diffraction patterns using Bragg's law. The specimens were oriented to maximize diffraction intensity so as to minimize deviation from the Bragg condition when recording SAED patterns. This generally limits the uncertainty of the lattice parameter measurements to approximately $\pm$ 0.3 per cent. Several diffraction patterns were taken from the Si substrate to calibrate the camera constant. Error bars in the figures were defined by the average range between maximum and minimum lattice parameters in each specimen.

Vertical spacings were obtained from diffraction patterns that were derived by fast Fourier transformation (FFT) of the digitized lattice fringe images. The pattern derived by FFT avoided the superlattice spots by using only a single Mo layer in the analysis. The lattice fringe images on the photographic plates were digitized using a CCD camera connected to a computer. Well-defined fringes were observed predominantly in the lateral direction due to the texturing of the Mo ($\langle 110 \rangle$ in the vertical direction). A 5 nm by 5 nm area over a layer, showing well defined {110} lattice fringes parallel to the interface, was chosen for FFT. The FFT of the periodic {110} lattice fringes resulted in sharp 110 diffraction spots in the vertical direction. An iterative procedure was used to determine the maximum intensity of each spot. Lattice fringes and corresponding FFT patterns of the Si substrate in the same image were used to calibrate the camera constant. FFT thus provides stresses in a "*single*" grain rather than numerous grains within a relatively large volume.

In order to supplement the FFT technique, which utilizes perforated thin foils, vertical elastic strains were also measured with an X-ray diffractometer with a CuK_α source ($\lambda = 0.154$ mm). The X-ray measurements were performed in the θ–2θ geometry on a Rigaku DMAX-IIB diffractometer (instrumental resolution of 0.1°). The specimens were scanned from $2\theta = 36°$ to 46° to include the Mo {110} peak. Due to a slight asymmetric peak shape, the peak position was determined at the strongest intensity. The asymmetry was negligible at times less than 5 h. At longer annealing times, using full-width-half maximums averages would increase the magnitude of strains by a factor of 1.2–1.3.

Supplementary techniques to the electronic diffraction and FFT measurements were considered important since perforation of a TEM thin foil by ion milling may affect the stress state. These measurements were performed at Arizona State University to an accuracy of $\pm$ 0.6%.

The wafer curvature measurements were performed using a laser deflectometer at Stanford University, described in detail elsewhere [10] and Tohoku University in Sendai, Japan. The analysis of curvature and the associated stresses in layers deposited on substrates is described by Townsend *et al.* [10]. The stress in a film, for a film thickness much less than the substrate thickness, is given by:

$$\sigma = \frac{E_s t_s^2}{6(1-\nu_s)t} K \quad (1)$$

where σ is the stress in the plane of the film, $M_{\langle 100 \rangle} = C_{11} + C_{12} - 2C_{12}^2/C_{11}$, $E_s/(1-\nu_s)$ is the biaxial modulus $= M_{\langle 100 \rangle}$, ν_s is the Poisson's ratio of the substrate, t_s is the substrate thickness, t is the film thickness and K is the change in substrate curvature due to elastic misfit with the adhering film. In thick (0.1 μm) films of a-Si, Mo on a-Si (Mo/a-Si) and a-Si on Mo/a-Si (a-Si/Mo/a-Si), the stress in each layer was determined by measuring the change in curvature after the deposition of each layer ($MoSi_2$ is very thin in comparison to the Mo and Si layers).

3. Results and discussion

An HREM image of an as-deposited multilayer is illustrated in Fig. 1a. The dark layers are Mo and the faint layers are a-Si. An intermediate shade of the amorphous a-Mo–Si interlayers is between these layers. The average Mo layer thickness was 2.33 nm and the average a-Si layer thickness was 3.06 nm for unannealed or "as-deposited" multilayers. The amorphous Mo–Si interlayers were 0.5 nm thick when Si was deposited on Mo and 1 nm thick when Mo was deposited on Si. An explanation for the difference in thicknesses of the interlayers is unclear, although others have also observed this disparity [11, 12]. Lattice fringes approximately parallel to the interfaces, corresponding to {110} type planes, are observed in the Mo layers. This indicates texturing with $\langle 110 \rangle$ directions perpendicular to the deposition plane, as mentioned in the previous section. Lateral grain dimensions of the Mo polycrystal vary from about 5 to 30 nm.

Fig. 1b–d shows a multilayer after 1 to 100 h anneals at 316°C. The Mo-a–Si interlayer thicknesses have increased with annealing time. Earlier work by the authors showed that the decreases in thickness of the Mo and a-Si layers was consistent with the increase in the amorphous interlayer thickness providing a Mo:Si stoichiometry of 1:2 (and that the densities of crystalline and amorphous Mo–Si are nearly equal) [3]. Thus, the stoichiometry of the amorphous Mo–Si is probably 1:2.

The growth of the thick (Mo on a-Si) interlayer as a function of annealing time is shown in Fig. 2. The thick interlayer rapidly grows from 1 to 1.4 nm in less than 1 h, then gradually grows to 1.8 nm by 50 h. The thin (a-Si on Mo) interlayer behaves similarly, with relatively rapid growth from 0.5 to 0.8 nm within 1 h, followed by gradual growth to 1.0 nm over 50 h. The secondary, gradual-growth stage, has been shown to be controlled by the diffusion of Si through the interlayer

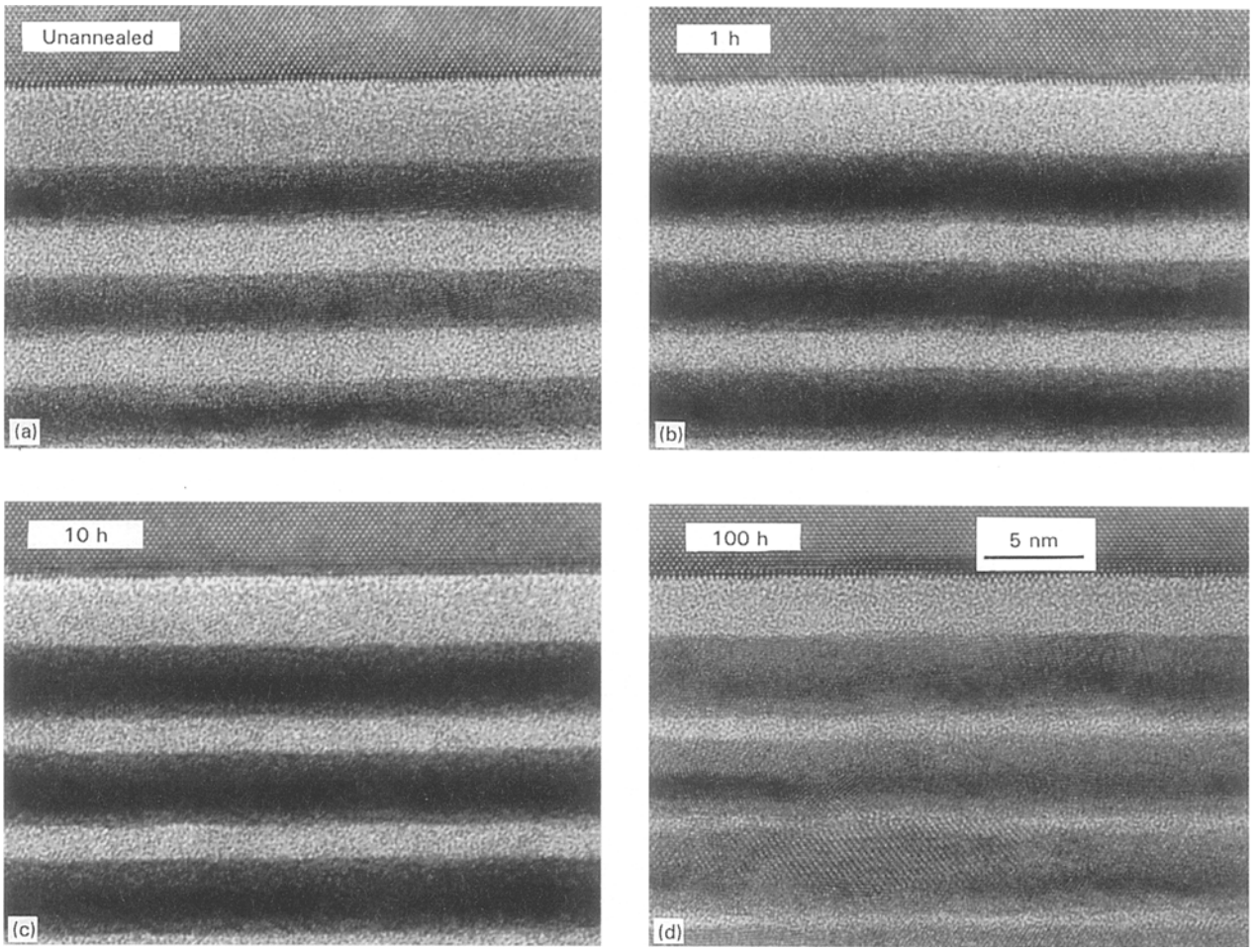

Figure 1 HREM images of (a) as-deposited Mo/a-Si multilayer, (b) multilayer annealed for 1 h at 316 °C, (c) 10 h at 316 °C, (d) 100 h at 316 °C.

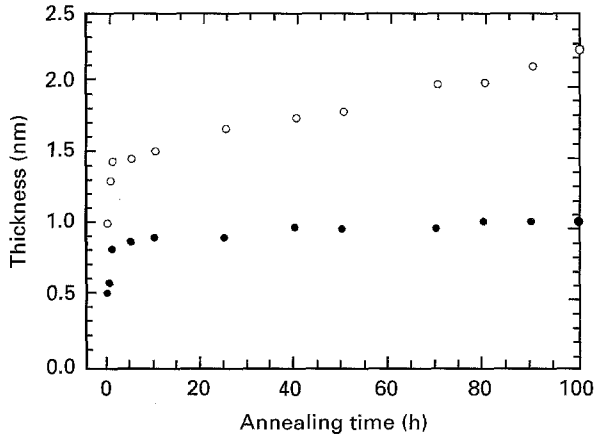

Figure 2 Growth of the interlayer during annealing at 316 °C. Open circles correspond to the thickness of the initially thicker amorphous Mo-Si interlayer (Mo deposited on Si). Filled circles are the thickness of the initially thinner interlayer (Si deposited on Mo). ○ thick interlayer; ● thin interlayer.

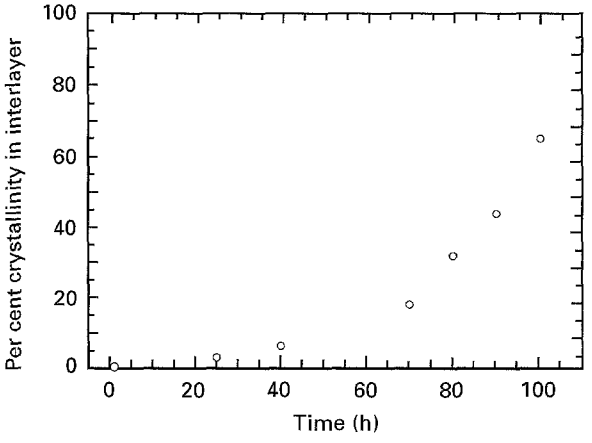

Figure 3 The variation in per cent crystallized amorphous Mo-Si (as observed in HREM images) as a function of annealing time.

to the Mo layer [1,2,13–15]. Crystalline hexagonal (h-) $MoSi_2$ forms during annealing [3]. Fig. 3 shows the volume fraction of the crystallized $MoSi_2$ as a function of annealing time. These are based on area fractions crystallized as determined from the HREM images. Since some crystallites were not oriented to exhibit lattice fringe contrast, the values in the figure are probably lower than the actual fraction of the crystallites. After about 100 h, the interlayers appear to have nearly completely transformed to h-$MoSi_2$, although only 80 per cent crystallization was confirmed. The crystallized volume after 50 h of annealing is only 10 per cent. As will be discussed subsequently, these results suggest that the effects of crystallization are not of primary importance in residual stress development.

Fig. 4a and b show the lateral Mo $(01\bar{1})$ and (100) lattice spacings in optical multilayers, determined by SAED as a function of annealing time. There is less (100) data due to uncertainty of (100) reflection images.

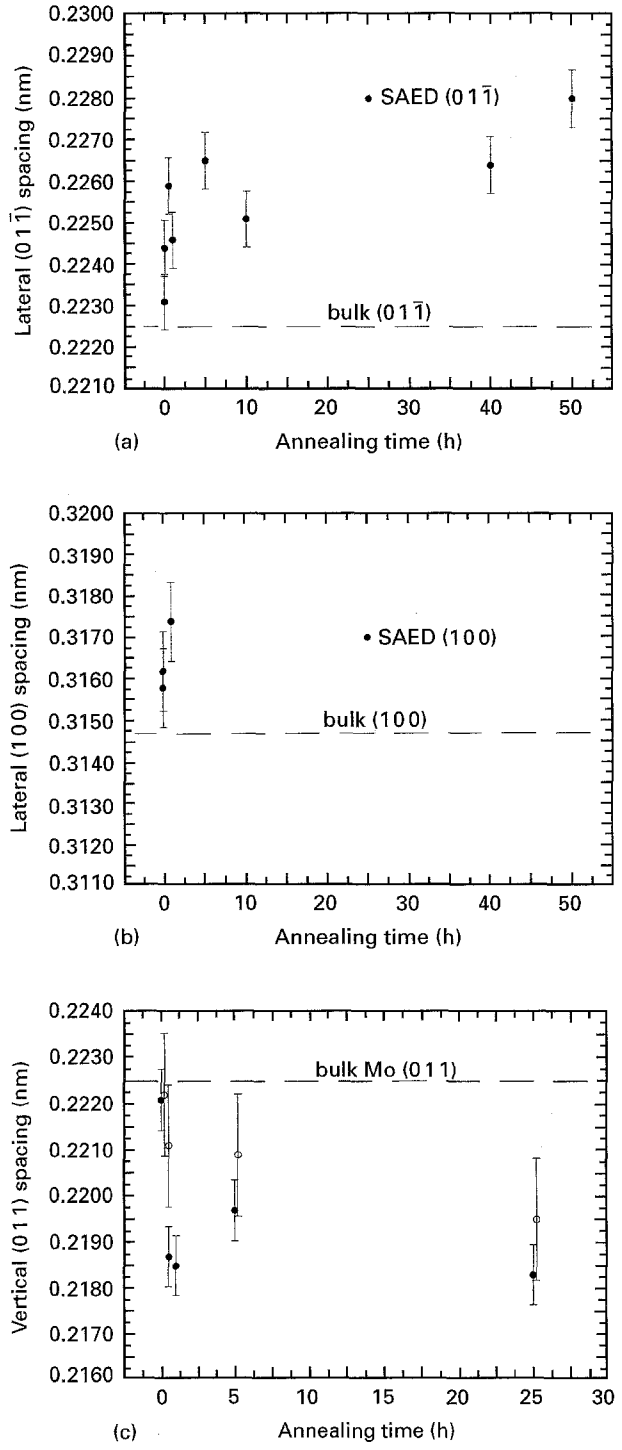

Figure 4 Variation of the Mo (a) (0 1 $\bar{1}$) and (b) (1 0 0) lateral lattice plane spacings during annealing at 316 °C; and (c) (0 1 1) vertical lattice plane spacings determined by SAED, HREM/FFT (●) and X-ray diffraction (XRD) (○).

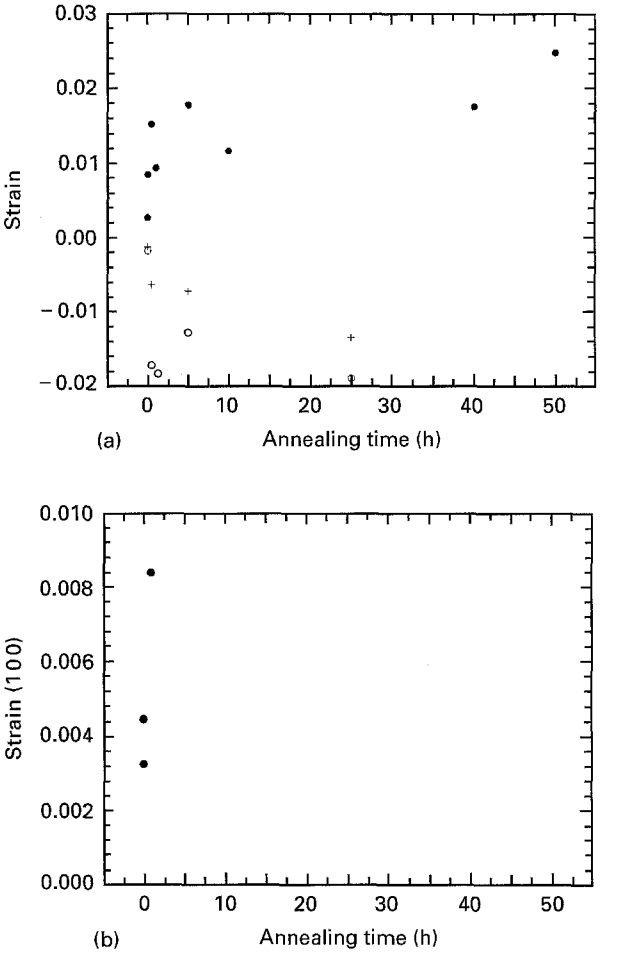

Figure 5 Variation in the vertical and in-plane strains of molybdenum in optical multilayers based on lattice plane spacings in Fig. 4. (a) refers to lateral (0 1 $\bar{1}$) spacings and vertical (0 1 1) spacings (or $\varepsilon_{[0\,1\,\bar{1}]}$). ● SAED (0 1 $\bar{1}$); ○ HREM (FFT (0 1 1)); + XRD (0 1 1). (b) refers to lateral (1 0 0) spacings (or $\varepsilon_{[1\,0\,0]}$).

TABLE I Stress (lateral) in thick (approx. 0.1 μm) layers as measured by laser deflectometry (MPa) before and after annealing at 316 °C

	(MPa)		
	Unannealed	Annealed 0.5 h	Annealed 10 h
a-Si on SiO_2 of Si substrate (0.11 μm)	− 1360	− 533	− 379
Mo on a-Si on substrate (0.105 μm)	+ 1140	+ 826	+ 834
a-Si on Mo (on a-Si on substrate (0.11 μm)	− 1242	− 30	− 190

Fig. 4c shows the vertical (011) spacing determined using HREM/FFT and XRD, also as a function of annealing time. The HREM/FFT and XRD are in reasonable agreement at longer times, although the lattice parameters from the latter technique may predict smaller strains. The dashed line is the spacing for bulk, unstressed, Mo. There is a rapid increase in lateral lattice parameter during the first 5 h followed by a more gradual increase. The vertical lattice spacing behaves similarly but with a compressive rather than a tensile sense. The associated stresses will be discussed later. Fig. 5a and b show the lateral and vertical strains versus annealing times based on the data of Fig. 4. The fact that the FFT strains are larger in magnitude than the XRD strains suggests that excessive relaxation in TEM thin foils is probably not occurring.

The stresses in the thick (0.1 μm) layers, as measured by deflectometry are listed in Table I. Significant compressive stresses in the amorphous silicon (deposited on SiO_2 of the silicon substrate) decrease with annealing, consistent with the findings by others [4, 16].

Interestingly, our "layered" 0.1 μm a-Si has a residual stress comparable [6] to that of single thin films of comparable thickness to our (3 nm) layers in our optical multilayer. The stress in the Mo layer deposited on a-Si is tensile in the lateral direction as with the multilayer case. However, relaxation occurs in the thick "layered film" in contrast to the thin Mo layers of the optical multilayer. The stress relaxation in 0.1 μm a-Si layer deposited on Mo is comparable for α-silicon on SiO_2.

The as-deposited multilayers have thin amorphous interlayers at the Mo/a-Si interfaces which grow during annealing. The growth is relatively rapid in the primary stage and slow in the secondary stage. Large tensile strains in the lateral direction in the thin (approximately 2.33 nm) Mo layers are present in the as-deposited multilayer and increase with annealing. There is also a corresponding contraction in the vertical direction.

The secondary growth stage, in both types of interlayers, has been shown in our earlier work [1, 2] to be a diffusion controlled process with an activation energy of 2.4 eV. This corresponds to the activation energy for Si diffusion in hexagonal (h-)$MoSi_2$ [14, 15, 17, 18]. While the mechanisms for the more gradual growth is understood in terms of classic diffusion, the explanation for the initial, rapid growth surge is less clear. It involves growth of only 1–2 atomic layers on each side of the amorphous MoSi interlayer. This rapid growth also appears to be thermally activated [1], and may be associated with the increase in Mo residual stress. Structural and/or composition changes in the interlayers cannot be easily assessed due to the amorphous nature and the very small dimensions. The relative speed of the short-range growth may imply that the Mo and Si atoms adjacent to the Mo/Mo-a-Si interfaces are "incorporated" into the interlayer by rate-dependent atomic rearrangements and are different than those of the later, long-range diffusion of Si through the MoSi interlayer (e.g. different diffusion path, vacancy concentration, etc.). It is possible that part of the driving force for the surge is a rearrangement or reconstruction which results in a decrease in free energy with structural modification, kinetically facilitated by an increase in temperature. The as-deposited interlayer may have an initial stoichiometry and amorphous structure that is relatively unstable. The above is certainly speculative and we are not aware of a relevant precedent in the literature, although interlayer formations (sometimes by amorphization) have been frequently observed (e.g. [19, 20]).

A single crystal Mo film with a (011) plane parallel to the film plane will have anisotropic elastic properties in the plane of the film [5]. The stresses in two perpendicular directions in the plane of the film, $\sigma_{[100]}$ and $\sigma_{[01\bar{1}]}$, can be calculated by:

$$\sigma_{[100]} = C_{11}\varepsilon_{[100]} + C_{12}\varepsilon_{[01\bar{1}]} - \frac{2C_{12}^2\varepsilon_{[100]} + C_{12}(C_{11} + C_{12} - 2C_{44})\varepsilon_{[01\bar{1}]}}{(C_{11} + C_{12} + 2C_{44})} \quad (2)$$

$$\sigma_{[01\bar{1}]} = C_{12}\varepsilon_{[100]} + \frac{(C_{11} + C_{12} + 2C_{44})}{2}\varepsilon_{[01\bar{1}]} - \frac{2C_{12}\varepsilon_{[100]} + (C_{11} + C_{12} - 2C_{44})\varepsilon_{[01\bar{1}]}}{2} \frac{(C_{11} + C_{12} - 2C_{44})}{(C_{11} + C_{12} + 2C_{44})} \quad (3)$$

where C_{11}, C_{12}, and C_{44} are the stiffness constants for Mo. These values are, respectively, 470, 168, and 107 GPa for bulk Mo [21]. (Our small (5–30 nm) crystals and the absence of an observed in-plane texture may imply that these stresses are similar. It will be shown later that our observed Poisson's ratio is supportive of such a similarity.)

The lateral Mo stress $\sigma_{[100]}$ is 2004 MPa while $\sigma_{[01\bar{1}]}$ was calculated at 1237 and 3096 MPa for the as-deposited multilayers. $\sigma_{[01\bar{1}]} = 6195$ MPa at 0.5 h. With 1 h annealing, $\sigma_{[100]}$ increases to 4144 and $\sigma_{[01\bar{1}]}$ to 3713 MPa. At 5 h $\sigma_{[01\bar{1}]} = 7288$ MPa. With 10 h and 50 h, $\sigma_{[01\bar{1}]}$ is 4737 and 10690 MPa, respectively, assuming $\varepsilon_{[01\bar{1}]} \simeq \varepsilon_{[100]}$ ($\varepsilon_{[100]}$ has a relatively small effect on $\sigma_{[01\bar{1}]}$ for comparable strain values). Since, as will be shown when Poisson ratios are discussed, the higher as-deposited $\varepsilon_{[01\bar{1}]}$ strain is anomalous, the lower as-deposited $\sigma_{[01\bar{1}]}$ value in Mo may be more reliable. These are all based on the lateral strains indicated in Fig. 5a and b. The stress in the unannealed 0.1 μm Mo layer was measured from laser deflectometry to be 1140 MPa. This is comparable to one (probably the more accurate) of the as-deposited stresses, indicating that adsorbed H_2O may not have an effect on the stress and also that activation of dislocation sources in thicker films ("layered") is not important at "*ambient temperature*". The decrease in tensile stress with annealing the 0.1 μm Mo layers may have been due to thermal activation of dislocation sources [5]. It has been shown that thicker layers, above the critical thickness (e.g. > 5 nm), allow for such sources [5]. Additionally, thermal activation may facilitate dislocation activity in "layered" films at elevated temperatures. Again, we expect the residual stresses in thin and thick amorphous Si layers to be equal because of the absence of the dislocation relaxation mechanism, also providing the absence of differences due to H_2O adsorption with each deposition pass and any change in structure (such as bulk defects with film thickness).

The data of Table I show that a-Si deposited on Mo and a-Si on SiO_2 have similar (unannealed) residual stresses at about −1300 MPa. The near equivalence suggests that at least for thick layers (and, perhaps, thin layers), despite the thickness and growth-rate differences between the a-Mo–Si interlayers for Mo deposited on a-Si and a-Si deposited on Mo, the nature of the interfaces, in terms of structural features that lead to residual strains, appears identical. (i.e. the data shows that for "free standing" Mo on Si and Si on Mo, the residual stresses are nearly the same.)

Table II shows the measured residual stress in 40 bilayer multilayers as a function of annealing time. The as-deposited multilayer residual stress of about −450 MPa is in good agreement with other work on

TABLE II Residual stresses in 40 bilayer optical multilayers versus annealing time at 316 °C determined from laser deflectometry

Annealing time (h)	Residual stress (MPa)
0.0	− 457
0.33	− 15 312
0.67	+ 2066
1.0	+ 1495
5.0	+ 1612
25.0	+ 1733

TABLE III "Theoretical" Poisson's ratio at various annealing times based on Equations 4 and 5

Annealing time (h)	$\varepsilon_{[0\,1\,1]}/\varepsilon_{[1\,0\,0]}$	$\varepsilon_{[0\,1\,1]}/\varepsilon_{[0\,1\,\bar{1}]}$
0	− 0.70	− 1.14
0	− 1.81[c]	− 0.64[c]
1/2	− 0.89[b]	− 0.89
1	− 0.96	− 0.85
5	− 0.89[b]	− 0.89
Average[a]	− 0.86	− 0.88

[a] $\varepsilon_{[0\,1\,1]}/\varepsilon_{[1\,0\,0]} = -1.81$ omitted.
[b] $\varepsilon_{[1\,0\,0]}$ assumed equal to $\varepsilon_{[0\,1\,\bar{1}]}$.
[c] Anomalously high and low values suggest erroneous stress (lattice parameter) measurements.

Mo–Si multilayers of similar period and thickness on (1 1 1) oriented silicon substrates [6, 7]. It can be noticed that the residual stress changes from about − 450 MPa, for the as-deposited multilayer, to between + 1500 and + 2000 MPa with annealing (an anomalously high compressive stress of − 15 312 MPa was observed after 20 min annealing). The amorphous silicon in the as-deposited 0.1 μm layer is under a + 1360 MPa residual stress. If the silicon layer is 3.06 nm thick, molybdenum is 2.33 nm thick and $MoSi_2$ ($MoSi_2$ between Mo deposited on Si plus $MoSi_2$ between Si deposited on Mo) is 1.5 nm thick, then the stress in the $MoSi_2$ is about − 1800 MPa. After about 0.5 h annealing this changes to about − 547 MPa and + 763 MPa after 10 h. This assumes multilayer and Mo layer stresses based on interpolation. (The anomalous 40 bilayer residual stress of about − 15 GPa would seem to imply an a-$MoSi_2$ stress of about − 40 GPa, which also appears anomalous).

The ratio of the expected vertical strain to lateral strain based on a "Poisson contraction" can be calculated assuming that the Mo layers are monocrystalline, with a ⟨1 1 0⟩ direction perpendicular to the deposition plane. The ratios of vertical strains to lateral strains in this coordinate system are:

$$\frac{\varepsilon_{[0\,1\,1]}}{\varepsilon_{[1\,0\,0]}} = \frac{-4C_{12}C_{44}\sigma_{[1\,0\,0]} - (C_{11}^2 + C_{11}C_{12} - 2C_{12}^2 - 2C_{11}C_{44})\sigma_{[0\,1\,\bar{1}]}}{4C_{44}(C_{11} + C_{12})\sigma_{[1\,0\,0]} - C_{12}\sigma_{[0\,1\,\bar{1}]})} \quad (4)$$

$$\frac{\varepsilon_{[0\,1\,1]}}{\varepsilon_{[0\,1\,\bar{1}]}} = \frac{-4C_{12}C_{44}\sigma_{[1\,0\,0]} - (C_{11}^2 + C_{11}C_{12} - 2C_{12}^2 - 2C_{11}C_{44})\sigma_{[0\,1\,\bar{1}]}}{-4C_{12}C_{44}\sigma_{[1\,0\,0]} + (C_{11}^2 + C_{11}C_{12} - 2C_{12}^2 - 2C_{11}C_{44})\sigma_{[0\,1\,\bar{1}]}} \quad (5)$$

where C_{11}, C_{12}, and C_{44} are the stiffness constants at ambient temperature from [21]. Table III shows the expected values based on Equations 4 and 5 (using stresses from Equations 2 and 3. Average values of $\varepsilon_{(1\,1\,0)}/\varepsilon_{(1\,0\,0)}$ and $\varepsilon_{(1\,1\,0)}/\varepsilon_{(0\,1\,\bar{1})}$ (ignoring the anomalous − 1.81 for one of the as-deposited lateral measurements) are between 0.85 and 0.90. Fig. 6a and b illustrate the observed Poisson's ratio values. The "*observed*" values are within reasonable agreement with expected or "theoretical values". These figures also illustrate the Poisson's ratio for the cases where the stresses are independent of the direction in the multilayer plane (iso-stress). The fact that the observed values of Poisson's ratio are close to the iso-stress value suggests that the stresses may be approximately independent of direction within the plane.

One concern, of course, is that the lattice parameter of an unstressed Mo film is not the same as that of bulk Mo [22]. Sources of deviation could include dissolution of Si into Mo. Of course, if the lattice distortions we observed were due to the strain field of point defects, then the vertical and lateral strains would be both positive (and of the same magnitude for spherically symmetric substitutional defects). This is clearly not the case here, as vertical strains are of opposite sign and are of a reasonable ratio for lattice parameter changes induced by interfacial constraints. It, thus, appears that point defects are not a significant influence on the unstressed lattice parameter. This is also consistent with the binary phase diagram data [23] that suggests that the solubility of Si in Mo at 316°C is, essentially, zero.

As discussed earlier, Kola *et al.* [4] suggested a plasticity mechanism facilitated by elevated temperature to rationalize the amorphous silicon film relaxation we also observed. The question remained, however, as to the cause of the increase in tensile stress/strain in the thin Mo layers with annealing that these investigators failed to observe. One possible explanation is that the increase is due to the relaxation of compression stress in the amorphous Si layers [2] as shown in Table I. However, the decrease in elastic strain energy in the Si layers is probably "consumed" by plastic deformation, which includes defect creation or annihilation and thermal losses in a-Si. As shown in Table IV, the elastic strain energy decrease in a-Si is comparable to the elastic strain energy increase in Mo. This suggests, therefore, that some other mechanism than a-Si relaxation by plasticity is involved in establishing large tensile stresses in thin Mo layers in annealed optical multilayers.

Various studies have been performed [24, 25] that observed an exothermic reaction with annealing a-Si at elevated temperatures. The heat released due to relaxation was about 4 kJ mol^{-1}, which yields

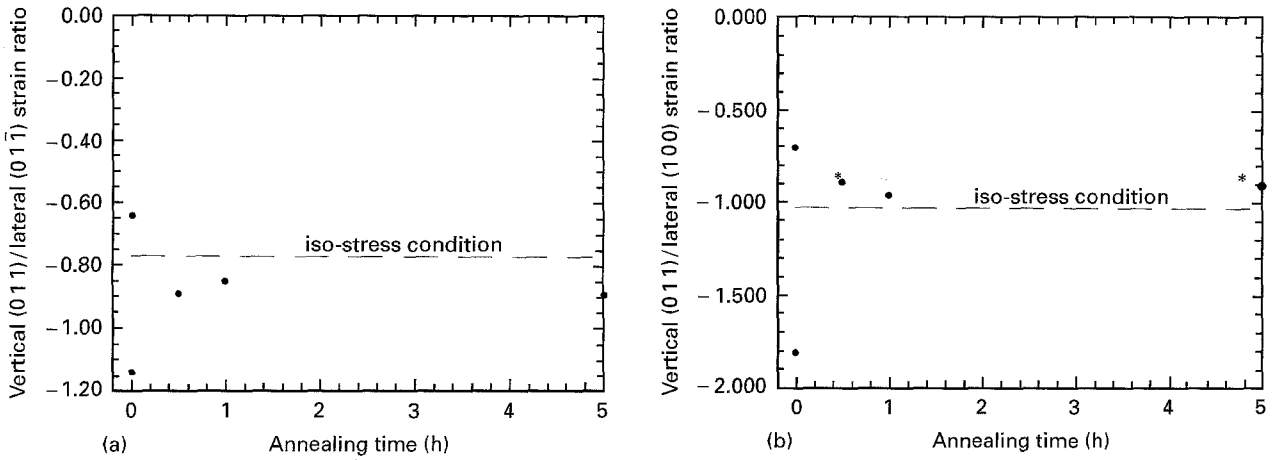

Figure 6 The vertical [(0 1 1)] and lateral [(1 0 0)] and (0 1 $\bar{1}$)] of Mo lattice spacings strain ratios during annealing at 316 °C as a function of annealing time. * indicates assumed iso-strain.

TABLE IV Change in elastic stress and strain energy in 40 thin layers of optical multilayers

	a-Si		Mo	
	Unannealed	Annealed 10 h	Unannealed	Annealed 10 h
Stress (average)	− 1494 MPa[a]	− 417 MPa[a]	2076 (1620) MPa[c]	4754 MPa
Biaxial modulus (average)	140 GPa		445 GPa[b]	
Thickness	3.06 nm	2.32 nm	2.33 nm	1.85 nm
Strain energy	1.03 J m^{-2}	0.06 J m^{-2}	0.43 J m^{-2}	2.6 J m^{-2}
Change in strain energy with annealing	–	− 0.91 J m^{-2}	–	+ 1.6 J m^{-2}

[a] Assumed equal to thick deposit of Table I.
[b] $(M_{\langle 1\,0\,0\rangle} + M_{\langle 1\,1\,0\rangle})/2$.
[c] $(\sigma_{[0\,1\,\bar{1}]} + \sigma_{[1\,0\,0]})/2$.
Note: Parentheses refer to stresses if anomalously high as-deposited Mo lattice parameter is omitted.

30 J m^{-2} in the 40 layers of a-Si. These values are substantially larger than the net elastic strain energy increase (see Table IV). This suggests sufficient energy to induce tensile stress at the interface. That is, changes in the a-Si (e.g. defect structure, bond angle [24, 26–28]) lead to changes at the interface which, in turn, lead to changes in the stress state. However, we have no direct evidence for a "phase change". It, perhaps, should be mentioned that these exothermic reactions in a-Si may be associated with the "plastic relaxation" in the a-Si described by Kola *et al.* [4].

Another explanation relates to the amorphous Mo–Si interlayers. As mentioned earlier, it is possible that the initial "growth surge" is evidence for a "reconstruction" or local structural change in the amorphous interlayer over a few atomic distances, which induces strains in the Mo and a-Si layers. This phase change or reconstruction is enabled, kinetically, at higher temperatures. It appears that the most pronounced stress increase is associated with the initial thickness "surge". The enthalpy of formation of $MoSi_2$ is 43.9 kJ mol^{-1} [29], and this is a typical value for the enthalpy of formation of Mo–Si compounds [29]. Although the enthalpy associated with a reconstruction is unknown, it may be comparable to the enthalpy of formation of Mo–Si compounds. The magnitude of the energy release by the formation of the thin $MoSi_2$ after the relatively rapid "thickness surge" to 0.8 and 1.44 nm with annealing at 316°C corresponds to an energy increase of about 173 J m^{-2} for 40 bilayers. Therefore, the driving force provided by the "surge" or reconstruction may be more than sufficient for the increase in the strain energy of the Mo layer ($\simeq$2 J m^{-2}).

Crystallization of the amorphous Mo–Si phase does not appear to explain the stress changes. The crystallized volume after 50 h annealing is only 10 per cent (after 100 h it is nearly 100 per cent). The residual stresses have reached a maximum at times less than 50 h.

4. Conclusions

1. Annealing of optical Mo–Si multilayers results in growth and crystallization of amorphous Mo–Si interlayers.

2. The thin (2–4 nm) layers of the as-deposited multilayer have substantial residual stresses + 1.2 to + 2.0 GPa in the Mo and about − 1.3 GPa in a-Si, based on HREM, SAED, XRD, and laser deflectometry methods. The $MoSi_2$ layers have an average residual stress of about − 1.8 GPa.

3. The residual stresses in the Mo increase to about 5 GPa, and in the a-Si decreases to about − 0.5 GPa

with 10 h annealing at 316°C. The $MoSi_2$ appears to increase to about + 0.8 GPa. The "total" residual stress in the optical multilayers increases substantially with 10 h annealing at 316°C from about − 450 to about + 2000 MPa.

4. Our results have similarities with some other work that suggests stress relaxation in amorphous silicon by plasticity. Tensile stresses increase relatively rapidly in the thin Mo layers. The source of this increase is also unclear, but may be associated with an observed relatively rapid growth in the amorphous Mo–Si interlayers. The growth may be associated with a local (about 0.3 nm) rearrangement/reconstruction of the a-(Mo–Si) interfaces leading to changes in the stress state of the Mo layers, although other sources, such as structural changes in the amorphous silicon or crystallization of the amorphous Mo–Si must be considered.

Acknowledgements

The authors wish to thank M. Villiardos for measurement of the interlayer thickness and Y. Cheng of Arizona State University for X-ray diffractometer experiments. We also wish to thank Professor W.D. Nix and V.T. Gillard for help with the Stanford laser deflectometer. The comments and discussion of the manuscript by T. Weihs of Johns Hopkins University and W. Johnson of Caltech are greatly appreciated. Portions of this work were performed under a subcontract from Lawrence Livermore National Laboratory to Oregon State University.

References

1. R. S. ROSEN, D. G. STEARNS, M. A. VILLIARDOS, M. E. KASSNER, S. P. VERNON and Y. CHENG, *Appl. Optics* **32** (1993) 6975.
2. R. S. ROSEN, D. G. STEARNS, M. E. KASSNER, J. KOIKE, Y. CHENG and S. P. VERNON, *J. Nano. Mater.* **3** (1993) 195.
3. D. G. STEARNS, R. S. ROSEN, and S. P, VERNON, Proceedings of the Multilayer Optics for Advanced X-Ray Applications, SPIE, **1547** (1991) 2.
4. R. R. KOLA, D. L. WINDT, W. K. WASKIEWCZ, B. E. WEIR, R. HULL, G. K. CELLAR and C. A. VOLKERT, *Appl. Phys. Lett.* **60** (1992) 3120.
5. W. D. NIX, *Metall. Trans.* **20A** (1989) 2217.
6. T. D. NGUYEN, *Mater. Res. Soc. Symp. Proc.* **343** (1994) 579.
7. T. D. NGUYEN, X. LU and J. H. UNDERWOOD, *Physics of X-Ray Multilayer Structures*, OSA Technical Digest Series **6** (1994) 102.
8. J .A. BAIN, L. J. CHYUNG, S. BRENNAN and B. M. CLEMENS, *Phys. Rev. B* **44** (1991) 1184.
9. D. G. STEARNS, R. S. ROSEN and S. P. VERNON, *J. Vac. Sci. Technol.* **A9** (1991) 2662.
10. P. H. TOWNSEND, D. M. BARNETT and T. A. BRUNNER, *J. Appl. Phys.* **62** (1987) 4438.
11. A. K. PETFORD-LONG, M. B. STEARNS, C.-H. CHANG, S. R. NUTT, D. G. STEARNS, N. M. CEGLIO and A. M. HAWRYLUK, *ibid.* **61** (1987) 1422.
12. K. HOLLOWAY, K. B. DO and R. SINCLAIR, *ibid.* **65** (1989) 474.
13. J. BAGLIN, J. DEMPSEY, W. HAMMER, F. D'HEURLE, S. PETERSON and C. SERANO, *J. Electron. Mater.* **8** (1979) 641.
14. J. Y. CHENG, H. C. CHENG and L. J. CHENG, *J. Appl. Phys.* **61** (1987) 2218.
15. P. R. GAGE and R. W. BARTLETT, *Trans. Metall. Soc. AIME* **233** (1965) 832.
16. A. WITVROUW and F. SPAEPEN, *Mater. Res. Symp. Proc.* **205** (1992) 21.
17. A. GUIVARC'H, P. AUVRAY, L. BERTHOU, M. LE CUN, J. P. BOULET, P. HENOC and G. PELOUS, *J. Appl. Phys.* **49** (1978) 233.
18. E. P. NECHIPORENKO, E. P. POLTASEV, N. S. KAPUSTIN, V. V. KAPUSTIN and YU T. KONDRATOV, *Izv. Akad. Nauk SSSR, Neorg. Mater.* **10** (1973) 1829.
19. T. SANDS and A. S. KAPLAN, *Appl. Phys. Lett.* **50** (1987) 1346.
20. F. Y. SHEAU and Y. A. CHANG, *ibid.* **55** (1989) 1510.
21. G. SIMMONS and H. WANG, "Single Crystal Elastic Constants and Calculated Aggregate Properties: A Handbook" 2nd Edn (The MIT Press, Cambridge, MA, 1971).
22. B. M. CLEMENS and J. A. BAIN, *MRS Bull.* **17** (1992) 46.
23. M. HANSEN and K. ANDERKO, "Constitution of Binary Alloys" (McGraw-Hill, New York, or General Electric Co., Business Growth Services, Schenectady, 1958).
24. S. ROORDA, W. C. SINKE, J. M. POATE, D. C. JACOBSON, P. FUOSS, S. DIERKER, B. S. DENNIS and F. SPAEPEN, *Mater. Res. Soc. Symp. Proc.* **157** (1990) 683.
25. S. ROORDA, S. DOORN, W. C. SINKE, P. M. L. O. SCHOLTE and E. VAN LOENEN, *Phys. Rev. Lett.* **62** (1989) 1880.
26. W. SINKE, T. WARABISAKO, M. MIYAO, T. TOKUYAMA, S. ROORDA and F. SARIS, *J. Non-Cryst. Solids* **39** (1988) 308.
27. R. TSU, J. GONZAREZ-HERNANDEZ and P. H. POLLAK, *ibid.* **66** (1984) 109.
28. *Idem, Solid State Commun.* **54** (1985) 447.
29. T. G. CHART, *Metal. Sci.* **8** (1974) 344.

Received 15 August
and accepted 17 October 1995